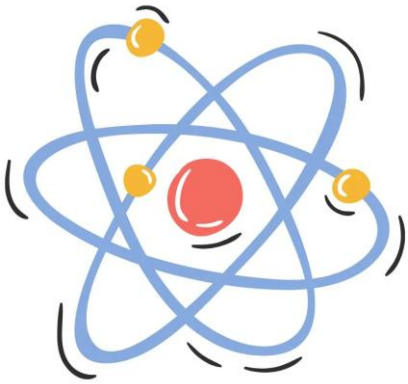

ISSN: 1672 - 6553

JOURNAL OF DYNAMICS AND CONTROL

VOLUME 10 ISSUE 05: P133-150

COMPUTATION OF BOND ADDITIVE TOPOLOGICAL CHARACTERIZATION OF NANO SHEETS BASED ON OCTA GRAPHENE

R. Vikram, V. Maheswari

Department of Mathematics, Vels Institute of Science, Technology & Advanced Studies (VISTAS), Chennai 600117, Tamil Nadu, India

JOURNAL OF DYNAMICS AND CONTROL
https://doi.org/10.71058/jodac.v10i05011

COMPUTATION OF BOND ADDITIVE TOPOLOGICAL CHARACTERIZATION OF NANO SHEETS BASED ON OCTA GRAPHENE

R. Vikram, V. Maheswari*

Department of Mathematics, Vels Institute of Science, Technology & Advanced Studies (VISTAS), Chennai 600117, Tamil Nadu, India

***Corresponding Author: maheswari.sbs@vistas.ac.in**

Contributing Author: vikymaths@gmail.com

Abstract: *Octa Graphene is a nanosheet made up of octagons and squares forming periodic unit cells. Owing to its exceptional physical and chemical properties, Octa Graphene has gained considerable interest in the fields of nano electronics and nano drug delivery. This study evaluates the topological characteristics of Octa Grayphyne and Octa Graphdine nanosheets using bond additive topological indices based on the degree concept. Some topological indices have been calculated in order to quantitatively study the structural behavior and molecular properties of the mentioned nanostructures. The findings offer valuable information regarding the stability, electronic, and vibrational properties of these nano materials. In addition, these nanostructures have shown great potential for use in nano-battery technology, drug delivery in cells, and advanced nano devices.*

Keywords: *Adriatic indices, Molecular graph, Octa-Grayphyne, Octa-Graphdine, Topological indices.*

1 Introduction

Nano sheets belong to 2D Nano structures. The carbon Nano sheets discovered in the last decade have attracted much interest among many scientists. They were obtained after heating the fibers at temperature above 350F for 24 hours. Graphene is a crystalline Nano structure made up of carbon atoms having strong bonds with only one atom thickness. While Graphene Nano sheets are 2D Nano structures made up of one layer of carbon atoms arranged in hexagonal lattices. Wu et al. [1] demonstrated that Graphene oxide sheet acts as a carrier of Adriamycin, which could reverse the drug resistance of breast cancer. Furthermore, it was reported that Graphene oxide sheets are also antineoplastic agents [2]. In conclusion, without any ambiguity, it is clear that Graphene oxide sheets help reduce deaths from cancer. 2D Nano sheets have brought about many possibilities to resolve the issue of water pollution caused by heavy metals in water through their utilization as a good candidate for the removal of heavy metal pollution from water. To learn more on nanosheets, you can refer to [3]. Octa Grephene is another type of Nano sheet of carbon made up of octagon and square structures. Poupitz et al. [4] introduce Octa-Grephyne and Octa-Graphdine Nano sheets. Before discussing these Nano sheets any further, it will be interesting to review the history of topological indices for chemical graphs; Molecular Descriptor is a way of translating chemical structure information into a numeric form. Topological Indices are one of the kinds of Molecular Descriptors. Topological Indices are numerical quantities derived from the graphic representation of chemical compounds. The importance of Topological Indices in QSAR lies in their ability to correlate psycho-chemical and bio- logical properties of chemical compounds. Harry Wiener was the pioneer in chemical graph theory. His research on Topolog- ical Indices is very radical and regarding QSAR approaches, one should refer to [5]. He came up with the idea of struc- ture-based invariants relating to the boiling points of paraffins. The Wiener

https://doi.org/10.71058/jodac.v10i05011

index introduced by him plays a vital role in nanotechnology.

Let $G = (V(G), E(G))$ be an graph. The number of peaks and verges in these collections is represented by their cardinality. $e = uv$ denotes an edge in $E(G)$ across end-to-end vertices. It is assumed that two vertices, u and v, are organized if there is a universal vertex between them. Mathematical chemical science is a branch of computational chemistry where, instead of using the principles of physics, we fight and forecast molecular structures using mathematical models. Graph theory is used to mathematically demonstrate chemical events in a branch of mathematical chemistry called "chemical graph theory" [6-8]. This idea had a significant impact on the evolution of the biochemical sciences.

A bond preservative descriptor Des can be inscribed as [9]

$$Des(G) = \sum_{uv \in E(G)} f(d_G(u), d_G(v))$$

where f is a mechanism that assigns an actual value to a well-ordered pair that contains a structure and is an edge, and $E(G)$ is the established of edges. Given that f might be narrow-minded in many conventions, it is clear that this has a rather broad connotation. The aforementioned topological indices are a group of molecular descriptors that are used to measure the structural properties of molecules. The degrees (or valences) of atoms in a molecular graph, represented as du and dv for two neighboring atoms u and v, provide the basis for calculating each index. Each index is explained in depth below, along with some possible uses:

S. No	Topological indices	Results
1	Randic-type lordeg index(RLI)	$ln(d_u) \times ln(d_v)$
2	Sum lordeg index(SLI)	$\sqrt{ln(d_u)} + \sqrt{ln(d_v)}$
3	Inverse sum lordeg index(ISLI)	$\frac{1}{\sqrt{ln(d_u)}+\sqrt{ln(d_v)}}$
4	Misbalance lordeg index(MLI)	$\lvert ln(d_u) - ln(d_v) \rvert$
5	Misbalance losdeg index(MLSI)	$\lvert ln^2 d_u - ln^2 d_v \rvert$
6	Misbalance indeg index(MII)	$\lvert \frac{1}{d_u} - \frac{1}{d_v} \rvert$
7	Misbalance irdeg index(MIRI)	$\lvert \frac{1}{\sqrt{d_u}} - \frac{1}{\sqrt{d_v}} \rvert$
8	Misbalance rodeg index(MRI)	$\lvert \sqrt{d_u} - \sqrt{d_v} \rvert$
9	Misbalance deg index(MDI)	$\lvert d_u - d_v \rvert$
10	Misbalance hadeg index(MHI)	$\lvert \left(\frac{1}{2}\right)^{d_u} - \left(\frac{1}{2}\right)^{d_v} \rvert$
11	Minimum-maxi rodeg index(MMRI)	$\sqrt{\frac{min(d_u,d_v)}{max(d_u,d_v)}}$
12	Max-minirodeg index(MMRDI)	$\sqrt{\frac{max(d_u,d_v)}{min(d_u,d_v)}}$
13	Max-minideg index(MMDI)	$\frac{max(d_u,d_v)}{min(d_u,d_v)}$

https://doi.org/10.71058/jodac.v10i05011

14	Max-minisdeg index(MMSDI)	$\left(\frac{max(d_u,d_v)}{min(d_u,d_v)}\right)^2$
15	Symmetric division deg index(SDDI)	$\frac{min(d_u,d_v)}{max(d_u,d_v)}+\frac{max(d_u,d_v)}{min(d_u,d_v)}$

The beneficial resources that graph theory offers for learning about substances theoretically are topological indices [10-19].

2 Main Results

2.1 Octa Graphyne Nanosheet

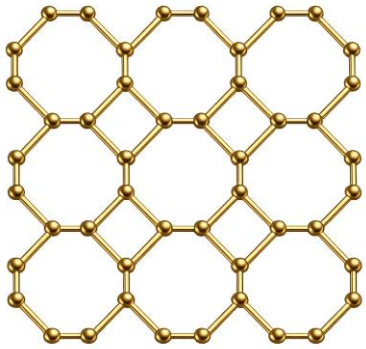

Figure 1: Graph of Octa graphyne nanosheet

Consider $O_1\ G_{(s\times t)}$ Octa Graphyne Nano sheet with s number of hexagons in each row and t hexagons in each column. From the graphical illustration of Octa- Graphyne nano sheet, it can be seen that every row of $O_1\ G_{(s\times t)}$ contains s hexagons and $s+1$ squares. The graph of $O_1\ G_{(s\times t)}$ is given in Figure 1. Similarly, in $O_1\ G_{(s\times t)}$, each consecutive column contains t hexagons and $t+1$ squares. Degree based indices are computed from degrees of end vertices corresponding to all edges. In $O_1\ G_{(s\times t)}$, there exist $4st+2s+2t$ number of vertices and $6st+s+t$ number of edges. On examining the graph of $O_1\ G_{(s\times t)}$, it can be noted that vertices of $O_1\ G_{(s\times t)}$ have either of degrees 2 or 3 by [20]. Based on the degrees of the vertices, edge partition of $O_1\ G_{(s\times t)}$ is given in Table 1.

Table 1: The Edge partition of Graph of Octa graphyne nanosheet

(d_u,d_v)	No. of Edges
(2,2)	$2s+2t+4$
(2,3)	$2s+2t-8$
(3,3)	$6st-5s-5t+4$

https://doi.org/10.71058/jodac.v10i05011

Theorem 1 *Let G_1 be a Octa Graphyne Nanosheet O_1 $G_{(s\times t)}$, then*

1. $RLI(G_1) = 7.2417st - 3.5519s - 3.5519t + 0.6616.$
2. $SLI(G_1) = 12.5832st - 3.3936s - 3.3936t.$
3. $ISLI(G_1) = 2.8608st - 0.1196s - 0.1196t + 0.0556.$
4. $MLI(G_1) = 0.8110s + 0.8110s - 3.2440.$
5. $MLSI(G_1) = 1.4530s + 1.4530s - 5.8120.$
6. $MII(G_1) = 0.3333s + 0.3333t - 1.3333.$
7. $MIRI(G_1) = 0.2594s + 0.2594t - 1.0376.$
8. $MRI(G_1) = 0.6358s + 0.6358t - 2.5432.$
9. $MDI(G_1) = 2s + 2t - 8.$
10. $MHI(G_1) = 0.25s + 0.25t - 1.$
11. $MMRI(G_1) = 6st - 1.3670s - 1.3670t + 1.4680.$
12. $MMRDI(G_1) = 6st - 0.5506s - 0.5506t - 1.7976.$
13. $MMDI(G_1) = 6st - 4.$
14. $MMSDI(G_1) = 6st + 1.5s + 1.5t - 10.$
15. $SDDI(G_1) = 12st - 1.6667s - 1.6667t - 1.3333.$

Proof.

$$RLI(G_1) = \sum_{uv\in E(G)} lnd_G(u)lnd_G(v)$$
$$= (ln2 \times ln2)(2s + 2t + 4) + (ln2 \times ln3)(2s + 2t - 8)$$
$$+(ln3 \times ln3)(6st - 5s - 5t + 4)$$
$$= 7.2417st - 3.5519s - 3.5519t + 0.6616.$$

$$SLI(G_1) = \sum_{uv\in E(G)} \sqrt{ln(d_u)} + \sqrt{ln(d_v)}$$
$$= \left[\sqrt{ln(2)} + \sqrt{ln(2)}\right](2s + 2t + 4) + \left[\sqrt{ln(2)} + \sqrt{ln(3)}\right](2s + 2t - 8)$$
$$+\left[\sqrt{ln(3)} + \sqrt{ln(3)}\right](6st - 5s - 5t + 4)$$
$$= 12.5832st - 3.3936s - 3.3936t.$$

$$ISLI(G_1) = \sum_{uv\in E(G)} \frac{1}{\sqrt{ln(d_u)}+\sqrt{ln(d_v)}}$$
$$= \left[\frac{1}{\sqrt{ln(2)}+\sqrt{ln(2)}}\right](2s + 2t + 4) + \left[\frac{1}{\sqrt{ln(2)}+\sqrt{ln(3)}}\right](2s + 2t - 8)$$
$$+\left[\frac{1}{\sqrt{ln(3)}+\sqrt{ln(3)}}\right](6st - 5s - 5t + 4)$$
$$= 2.8608st - 0.1196s - 0.1196t + 0.0556.$$

$$MLI(G_1) = \sum_{uv\in E(G)} |lnd_u - lnd_v|$$
$$= |ln2 - ln2|(2s + 2t + 4) + |ln2 - ln3|(2s + 2t - 8)$$
$$+|ln3 - ln3|(6st - 5s - 5t + 4)$$
$$= 0.8110s + 0.8110t - 3.2440.$$

$$MLSI(G_1) = \sum_{uv\in E(G)} |ln^2 d_u - ln^2 d_v|$$
$$= |ln^2 2 - ln^2 2|(2s + 2t + 4) + |ln^2 2 - ln^2 3|(2s + 2t - 8)$$

https://doi.org/10.71058/jodac.v10i05011

$$+|ln^2 3 - ln^2 3|(6st - 5s - 5t + 4)$$
$$= 1.4530s + 1.4530t - 5.8120.$$

$$MII(G_1) = \sum_{uv \in E(G)} \left|\frac{1}{d_u} - \frac{1}{d_v}\right|$$
$$= \left|\frac{1}{2} - \frac{1}{2}\right|(2s + 2t + 4) + \left|\frac{1}{2} - \frac{1}{3}\right|(2s + 2t - 8) + \left|\frac{1}{3} - \frac{1}{3}\right|(6st - 5s - 5t + 4)$$
$$= 0.3333s + 0.3333t - 1.3333.$$

$$MIRI(G_1) = \sum_{uv \in E(G)} \left|\frac{1}{\sqrt{d_u}} - \frac{1}{\sqrt{d_v}}\right|$$
$$= \left|\frac{1}{\sqrt{2}} - \frac{1}{\sqrt{2}}\right|(2s + 2t + 4) + \left|\frac{1}{\sqrt{2}} - \frac{1}{\sqrt{3}}\right|(2s + 2t - 8)$$
$$+ \left|\frac{1}{\sqrt{3}} - \frac{1}{\sqrt{3}}\right|(6st - 5s - 5t + 4)$$
$$= 0.2594s + 0.2594t - 1.0376.$$

$$MRI(G_1) = \sum_{uv \in E(G)} |\sqrt{d_u} - \sqrt{d_v}|$$
$$= |\sqrt{2} - \sqrt{2}|(2s + 2t + 4) + |\sqrt{2} - \sqrt{3}|(2s + 2t - 8)$$
$$+ |\sqrt{3} - \sqrt{3}|(6st - 5s - 5t + 4)$$
$$= 0.6358s + 0.6358t - 2.5432.$$

$$MDI(G_1) = \sum_{uv \in E(G)} |d_u - d_v|$$
$$= |2 - 2|(2s + 2t + 4) + |2 - 3|(2s + 2t - 8)$$
$$+ |3 - 3|(6st - 5s - 5t + 4)$$
$$= 2s + 2t - 8.$$

$$MHI(G_1) = \sum_{uv \in E(G)} \left|\left(\frac{1}{2}\right)^{d_u} - \left(\frac{1}{2}\right)^{d_v}\right|$$
$$= \left|\left(\frac{1}{2}\right)^2 - \left(\frac{1}{2}\right)^2\right|(2s + 2t + 4) + \left|\left(\frac{1}{2}\right)^2 - \left(\frac{1}{2}\right)^3\right|(2s + 2t - 8)$$
$$+ \left|\left(\frac{1}{2}\right)^3 - \left(\frac{1}{2}\right)^3\right|(6st - 5s - 5t + 4)$$
$$= 0.25s + 0.25t - 1.$$

$$MMRI(G_1) = \sum_{uv \in E(G)} \sqrt{\frac{mini(d_u, d_v)}{maxi(d_u, d_v)}}$$
$$= \sqrt{\frac{mini(2,2)}{maxi(2,2)}}(2s + 2t + 4) + \sqrt{\frac{mini(2,3)}{maxi(2,3)}}(2s + 2t - 8)$$
$$+ \sqrt{\frac{mini(3,3)}{maxi(3,3)}}(6st - 5s - 5t + 4)$$

https://doi.org/10.71058/jodac.v10i05011

$$= 6mn - 1.3670s - 1.3670t + 1.4680.$$

$$MMRDI(G_1) = \sum_{uv\in E(G)} \sqrt{\frac{maxi(d_u,d_v)}{mini(d_u,d_v)}}$$
$$= \sqrt{\frac{maxi(2,2)}{mini(2,2)}}(2s + 2t + 4) + \sqrt{\frac{maxi(2,3)}{mini(2,3)}}(2s + 2t - 8)$$
$$+ \sqrt{\frac{maxi(3,3)}{mini(3,3)}}(6st - 5s - 5t + 4)$$
$$= 6st - 0.5506s - 0.5506t - 1.7976.$$

$$MMDI(G_1) = \sum_{uv\in E(G)} \frac{maxi(d_u,d_v)}{mini(d_u,d_v)}$$
$$= \frac{maxi(2,2)}{mini(2,2)}(2s + 2t + 4) + \frac{maxi(2,3)}{mini(2,3)}(2s + 2t - 8)$$
$$+ \frac{maxi(3,3)}{mini(3,3)}(6st - 5s - 5t + 4)$$
$$= 6st - 4.$$

$$MMSDI(G_1) = \sum_{uv\in E(G)} \left(\frac{maxi(d_u,d_v)}{mini(d_u,d_v)}\right)^2$$
$$= \left(\frac{maxi(2,2)}{mini(2,2)}\right)^2 (2s + 2t + 4) + \left(\frac{maxi(2,3)}{mini(2,3)}\right)^2 (2s + 2t - 8)$$
$$+ \left(\frac{maxi(3,3)}{mini(3,3)}\right)^2 (6st - 5s - 5t + 4)$$
$$= 6st + 1.5s + 1.5t - 10.$$

$$SDDI(G_1) = \sum_{uv\in E(G)} \left[\frac{mini(d_u,d_v)}{maxi(d_u,d_v)} + \frac{maxi(d_u,d_v)}{mini(d_u,d_v)}\right]$$
$$= \left[\frac{mini(2,2)}{maxi(2,2)} + \frac{maxi(2,2)}{mini(2,2)}\right](2s + 2t + 4) + \left[\frac{mini(2,3)}{maxi(2,3)} + \frac{maxi(2,3)}{mini(2,3)}\right]$$
$$(2s + 2t - 8) + \left[\frac{mini(3,3)}{maxi(3,3)} + \frac{maxi(3,3)}{mini(3,3)}\right](6st - 5s - 5t + 4)$$
$$= 12st - 1.6667s - 1.6667t - 1.3333.$$

Figures 2 and 3 display the numerical values and graphical depictions of different bond-additive chemical descriptors for Octa Graphyne Nanosheet structures.

The behavior of the indices shown in Figure 2 can be explained by the numerical values in Table 2 . As the parameters s and t increase, all eight bond additive topological indices of the Octa Graphyne Nanosheet O_1 $G_{(s\times t)}$ increase steadily, though at different rates and patterns. $RLI(G)$ and $SLI(G)$ grow quickly and reach larger values. This is because they rely heavily on squared degree terms and edge contributions from nearby vertices. $RLI(G)$ increases more rapidly due to its greater sensitivity to rising vertex degrees in the expanding nanosheet structure. $ISLI(G)$

https://doi.org/10.71058/jodac.v10i05011

remains smaller and increases smoothly due to its balanced reliance on inverse and logarithmic degree terms. $MLI(G)$ and $MIRI(G)$ show moderate growth with steady increases as the structural connectivity rises. $MLSI(G)$ also grows sharply and reaches high values, as it greatly enhances the contribution of high-degree vertices. On the other hand, $MII(G)$ grows slowly and stays among the smallest indices across the range of s and t. $MRI(G)$ reaches medium-to-large values and increases consistently, surpassing $MLI(G)$ and $MIRI(G)$, but its growth is less aggressive than that of $RLI(G)$ and $MLSI(G)$. In the $3D$ graphical representation, the steeper surfaces correspond to indices that are sensitive to structural expansion, while flatter surfaces indicate slower and more stable growth. Overall, the graph shows that all indices are positively linked to the size, connectivity, and density of the Octa Graphene Nanosheet network.

Table 2: Calculated Bond Additive numerical value

(s, t)	$RLI(G_1)$	$SLI(G_1)$	$ISLI(G_1)$	$MLI(G_1)$	$MLSI(G_1)$	$MII(G_1)$	$MIRI(G_1)$	$MRI(G_1)$
(3, 3)	45	93	25	2	3	1	1	1
(4, 4)	88	174	45	3	6	1	1	3
(5, 5)	146	281	70	5	9	2	2	4
(6, 6)	219	412	102	6	12	3	2	5
(7, 7)	306	569	139	8	15	3	3	6
(8, 8)	407	751	181	10	17	4	3	8
(9, 9)	523	958	230	11	20	5	4	9
(10, 10)	654	1190	284	13	23	5	4	10
(11, 11)	799	1448	344	15	26	6	5	11
(12, 12)	958	1731	409	16	29	7	5	13

https://doi.org/10.71058/jodac.v10i05011

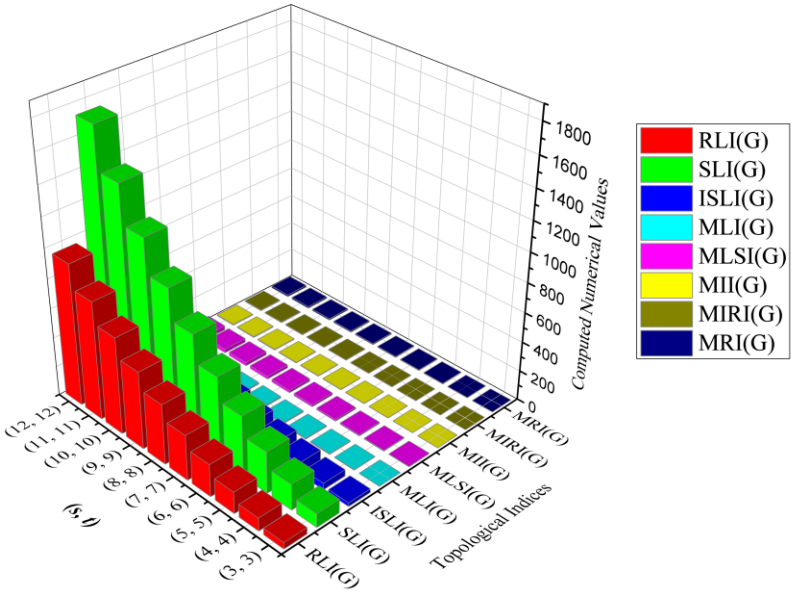

Figure 2: A visual representation of molecular characteristics for bond addition of Octa Graphene Nanosheet

The behavior of the indices shown in Figure 3 can be explained by the numerical values in Table 3. As the parameters s and t increase, all seven bond additive topological indices of O_1 $G_{(s\times t)}$ rise steadily, although they do so at different rates and magnitudes. $MDI(G)$ increases quickly from moderate to very large values. This index grows more than linearly because it is highly sensitive to increasing vertex degrees and edge density in the expanding nanosheet structure. $MHI(G)$ stays the smallest index throughout the range studied and grows very slowly, with only slight stepwise changes. This slow growth is due to its harmonic-type reciprocal degree contributions, which lessen the impact of high-degree vertices. $MMRI(G)$ is in the lower-to-middle range and increases smoothly. It shows moderate sensitivity to structural expansion. $MMRDI(G)$ sits in the middle range and grows steadily at a pace stronger than $MMRI(G)$, but weaker than the very sensitive SD-type indices. $MMDI(G)$ shows relatively strong growth and reaches higher values at larger s and t. This indicates its reliance on multiplicative degree interactions within the network. $MMSDI(G)$ is one of the largest and fastest-growing indices, with steep successive increases and high sensitivity to growing connectivity and the structural density of the nanosheet. $SDDI(G)$ also grows quickly and reaches high values, surpassing all middle-range indices and nearly matching the aggressive growth of $MMSDI(G)$. In the $3D$ graph, steeper surfaces correspond to indices that depend more on higher-order degree interactions. Flatter surfaces indicate slower and more stable growth. Overall, the graph shows that all seven indices are closely linked to the growing size, connectivity, and complexity of the Octa Graphene Nanosheet network.

https://doi.org/10.71058/jodac.v10i05011

Table 3: Calculated Bond Additive numerical value

(s, t)	$MDI(G_1)$	$MHI(G_1)$	$MMRI(G_1)$	$MMRDI(G_1)$	$MMDI(G_1)$	$MMSDI(G_1)$	$SDDI(G_1)$
(3, 3)	4	1	47	49	50	53	97
(4, 4)	8	1	87	90	92	98	177
(5, 5)	12	2	138	143	146	155	282
(6, 6)	16	2	201	208	212	224	411
(7, 7)	20	3	276	284	290	305	563
(8, 8)	24	3	364	373	380	398	740
(9, 9)	28	4	463	474	482	503	941
(10, 10)	32	4	574	587	596	620	1165
(11, 11)	36	5	697	712	722	749	1414
(12, 12)	40	5	833	849	860	890	1687

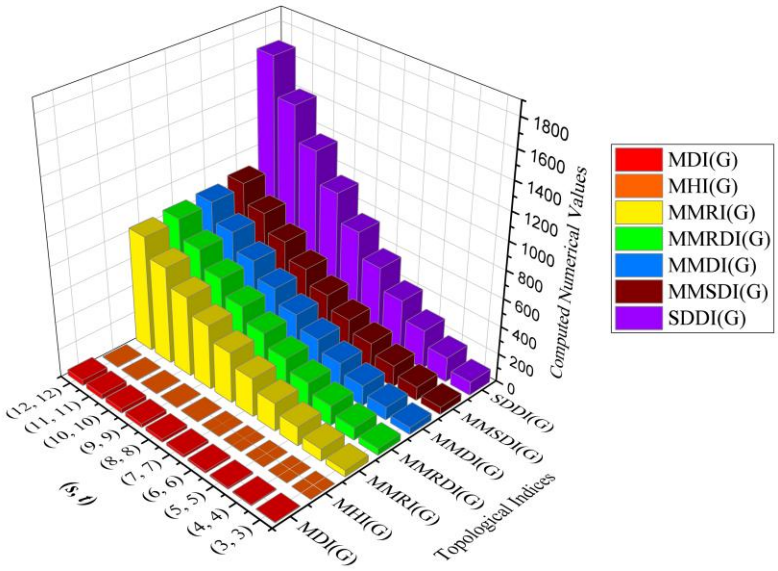

Figure 3: A visual representation of molecular characteristics for bond addition of Octa Graphene Nanosheet

https://doi.org/10.71058/jodac.v10i05011

2.2 Octa Graphdine Nanosheet

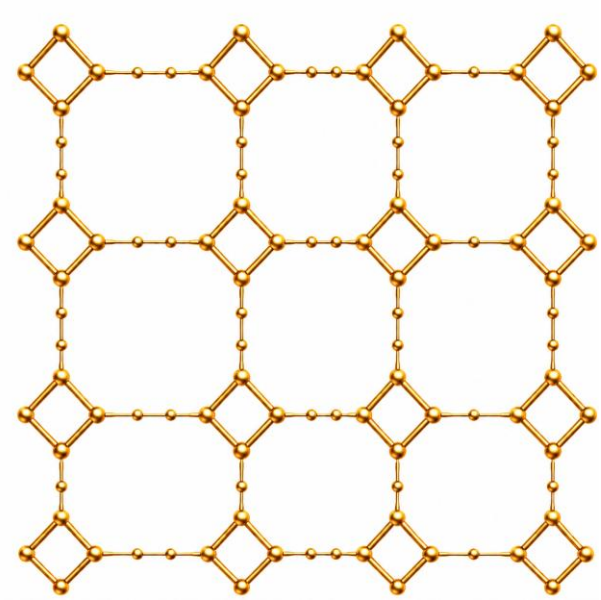

Figure 4: Graph of Octa Graphdine Nanosheet

Let $O_2\ G_{(s\times t)}$ be an Octa Graphdine Nanosheet with s hexadecagones having each row and t hexadecagones in each column. It is seen from the graph of the Octa-Grayphdine Nano sheet that there are s hexadecagones and $s+1$ squares in each row of $O_2\ G_{(s\times t)}$. The e graph of the Octa Graphdine Nanosheet $O_2\ G_{(s\times t)}$ is shown in Figure 4. In the same way, the number of columns in $O_2\ G_{(s\times t)}$ consists t hexadecagones and $t+1$ squares. Degree of end vertices for each edge is considered while evaluating the degree-based topological indices. The total number of vertices in $O_2\ G_{(s\times t)}$ is $8st+6s+6t+4$, whereas the number of edges in $O_2\ G_{(s\times t)}$ is $10st+7s+7t+4$. One can see from the graph of $O_2\ G_{(s\times t)}$ that all vertices in $O_2\ G_{(s\times t)}$ have a degree 2 or 3 (refer [20]). Edge partitioning depending on the degree of vertices is shown in Table 4.

Table 4: The Edge partition of Octa Graphdine Nanosheet

(d_u, d_v)	No. of Edges
(2,2)	$2st+s+t+4$
(2,3)	$4st+6s+6t$
(3,3)	$4st$

Theorem 2 *Let G_2 be a Octa Graphdine Nanosheet $O_2\ G_{(s\times t)}$, then*

1. $RLI(G_2) = 8.8327st + 5.0465s + 5.0465t + 1.9218.$
2. $SLI(G_2) = 19.2440st + 12.9524s + 12.9524t + 6.6608.$

https://doi.org/10.71058/jodac.v10i05011

3. $ISLI(G_2) = 5.2350st + 3.7907s + 3.7907t + 2.4020.$
4. $MLI(G_2) = 1.6220st + 2.4330s + 2.4330t.$
5. $MLSI(G_2) = 2.9060st + 4.3590s + 4.3590t.$
6. $MII(G_2) = 0.6667st + s + t.$
7. $MIRI(G_2) = 0.5188st + 0.7782s + 0.7782t.$
8. $MRI(G_2) = 1.2716st + 1.9074s + 1.9074t.$
9. $MDI(G_2) = 4st + 6s + 6t.$
10. $MHI(G_2) = 0.5st + 0.75s + 0.75t.$
11. $MMRI(G_2) = 9.2660st + 5.8990s + 5.8990t + 4.$
12. $MMRDI(G_2) = 10.8988st + 8.3482s + 8.3482t + 4.$
13. $MMDI(G_2) = 12st + 10s + 10t + 4.$
14. $MMSDI(G_2) = 15st + 14.5s + 14.5t + 4.$
15. $SDDI(G_2) = 20.6667st + 15s + 15t + 8.$

Proof.

$$RLI(G_2) = \sum_{uv\in E(G)} lnd_G(u)lnd_G(v)$$
$$= (ln2 \times ln2)(2st + s + t + 4) + (ln2 \times ln3)(4st + 6s + 6t)$$
$$+(ln3 \times ln3)(4st)$$
$$= 8.8327st + 5.0465s + 5.0465t + 1.9218.$$

$$SLI(G_2) = \sum_{uv\in E(G)} \sqrt{ln(d_u)} + \sqrt{ln(d_v)}$$
$$= \left[\sqrt{ln(2)} + \sqrt{ln(2)}\right](2st + s + t + 4) + \left[\sqrt{ln(2)} + \sqrt{ln(3)}\right]$$
$$(4st + 6s + 6t) + \left[\sqrt{ln(3)} + \sqrt{ln(3)}\right](4st)$$
$$= 19.2440st + 12.9524s + 12.9524t + 6.6608.$$

$$ISLI(G_2) = \sum_{uv\in E(G)} \frac{1}{\sqrt{ln(d_u)}+\sqrt{ln(d_v)}}$$
$$= \left[\frac{1}{\sqrt{ln(2)}+\sqrt{ln(2)}}\right](2st + s + t + 4) + \left[\frac{1}{\sqrt{ln(2)}+\sqrt{ln(3)}}\right]$$
$$(4st + 6s + 6t) + \left[\frac{1}{\sqrt{ln(3)}+\sqrt{ln(3)}}\right](4st)$$
$$= 5.2350st + 3.7907s + 3.7907t + 2.4020.$$

$$MLI(G_2) = \sum_{uv\in E(G)} |lnd_u - lnd_v|$$
$$= |ln2 - ln2|(2st + s + t + 4) + |ln2 - ln3|(4st + 6s + 6t)$$
$$+|ln3 - ln3|(4st)$$
$$= 1.6220st + 2.4330s + 2.4330t.$$

$$MLSI(G_2) = \sum_{uv\in E(G)} |ln^2 d_u - ln^2 d_v|$$
$$= |ln^2 2 - ln^2 2|(2st + s + t + 4) + |ln^2 2 - ln^2 3|(4st + 6s + 6t)$$

https://doi.org/10.71058/jodac.v10i05011

$$+|ln^2 3 - ln^2 3|(4st)$$
$$= 2.9060st + 4.3590s + 4.3590t.$$

$$MII(G_2) = \sum_{uv\in E(G)} \left|\frac{1}{d_u} - \frac{1}{d_v}\right|$$
$$= \left|\frac{1}{2} - \frac{1}{2}\right|(2st + s + t + 4) + \left|\frac{1}{2} - \frac{1}{3}\right|(4st + 6s + 6t) + \left|\frac{1}{3} - \frac{1}{3}\right|(4st)$$
$$= 0.6667st + s + t.$$

$$MIRI(G_2) = \sum_{uv\in E(G)} \left|\frac{1}{\sqrt{d_u}} - \frac{1}{\sqrt{d_v}}\right|$$
$$= \left|\frac{1}{\sqrt{2}} - \frac{1}{\sqrt{2}}\right|(2st + s + t + 4) + \left|\frac{1}{\sqrt{2}} - \frac{1}{\sqrt{3}}\right|(4st + 6s + 6t)$$
$$+ \left|\frac{1}{\sqrt{3}} - \frac{1}{\sqrt{3}}\right|(4st)$$
$$= 0.5188st + 0.7782s + 0.7782t.$$

$$MRI(G_2) = \sum_{uv\in E(G)} |\sqrt{d_u} - \sqrt{d_v}|$$
$$= |\sqrt{2} - \sqrt{2}|(2st + s + t + 4) + |\sqrt{2} - \sqrt{3}|(4st + 6s + 6t)$$
$$+|\sqrt{3} - \sqrt{3}|(4st)$$
$$= 1.2716st + 1.9074s + 1.9074t.$$

$$MDI(G_2) = \sum_{uv\in E(G)} |d_u - d_v|$$
$$= |2 - 2|(2st + s + t + 4) + |2 - 3|(4st + 6s + 6t) + |3 - 3|(4st)$$
$$= 4st + 6s + 6t.$$

$$MHI(G_2) = \sum_{uv\in E(G)} \left|\left(\frac{1}{2}\right)^{d_u} - \left(\frac{1}{2}\right)^{d_v}\right|$$
$$= \left|\left(\frac{1}{2}\right)^2 - \left(\frac{1}{2}\right)^2\right|(2st + s + t + 4) + \left|\left(\frac{1}{2}\right)^2 - \left(\frac{1}{2}\right)^3\right|(4st + 6s + 6t)$$
$$+ \left|\left(\frac{1}{2}\right)^3 - \left(\frac{1}{2}\right)^3\right|(4st)$$
$$= 0.5st + 0.75s + 0.75t.$$

$$MMRI(G_2) = \sum_{uv\in E(G)} \sqrt{\frac{mini(d_u,d_v)}{maxi(d_u,d_v)}}$$
$$= \sqrt{\frac{mini(2,2)}{maxi(2,2)}}(2st + s + t + 4) + \sqrt{\frac{mini(2,3)}{maxi(2,3)}}(4st + 6s + 6t)$$
$$+ \sqrt{\frac{mini(3,3)}{maxi(3,3)}}(4st)$$
$$= 9.2660st + 5.8990s + 5.8990t + 4.$$

https://doi.org/10.71058/jodac.v10i05011

$$MMRDI(G_2) = \sum_{uv\in E(G)} \sqrt{\frac{maxi(d_u,d_v)}{mini(d_u,d_v)}}$$
$$= \sqrt{\frac{maxi(2,2)}{mini(2,2)}}(2st + s + t + 4) + \sqrt{\frac{maxi(2,3)}{mini(2,3)}}(4st + 6s + 6t)$$
$$+ \sqrt{\frac{maxi(3,3)}{mini(3,3)}}(4st)$$
$$= 10.8988st + 8.3482s + 8.3482t + 4.$$

$$MMDI(G_2) = \sum_{uv\in E(G)} \frac{maxi(d_u,d_v)}{mini(d_u,d_v)}$$
$$= \frac{maxi(2,2)}{mini(2,2)}(2st + s + t + 4) + \frac{maxi(2,3)}{mini(2,3)}(4st + 6s + 6t) + \frac{maxi(3,3)}{mini(3,3)}(4st)$$
$$= 12st + 10s + 10t + 4.$$

$$MMSDI(G_2) = \sum_{uv\in E(G)} \left(\frac{maxi(d_u,d_v)}{mini(d_u,d_v)}\right)^2$$
$$= \left(\frac{maxi(2,2)}{mini(2,2)}\right)^2 (2st + s + t + 4) + \left(\frac{maxi(2,3)}{mini(2,3)}\right)^2 (4st + 6s + 6t)$$
$$+ \left(\frac{maxi(3,3)}{mini(3,3)}\right)^2 (4st)$$
$$= 15st + 14.5s + 14.5t + 4.$$

$$SDDI(G_2) = \sum_{uv\in E(G)} \left[\frac{mini(d_u,d_v)}{maxi(d_u,d_v)} + \frac{maxi(d_u,d_v)}{mini(d_u,d_v)}\right]$$
$$= \left[\frac{mini(2,2)}{maxi(2,2)} + \frac{maxi(2,2)}{mini(2,2)}\right](2st + s + t + 4) + \left[\frac{mini(2,3)}{maxi(2,3)} + \frac{maxi(2,3)}{mini(2,3)}\right]$$
$$(4st + 6s + 6t) + \left[\frac{mini(3,3)}{maxi(3,3)} + \frac{maxi(3,3)}{mini(3,3)}\right](4st)$$
$$= 20.6667st + 15s + 15t + 8.$$

The numerical values and graphical representations of various bond-additive molecular descriptors for Octa Graphdine Nanosheet structures are presented in Figure 5 and 6.

The behavior of the indices as depicted in Figure 5 can be explained using the numerical values presented in Table 5. As the parameters s and t increase, all eight bond-additive topological indices of the Octa Graphdine Nanosheet O_2 $G_{(s\times t)}$ increase monotonically, but with different magnitudes and growth patterns. $RLI(G)$ exhibits rapid growth and attains comparatively larger values because it strongly depends on higher-degree vertex interactions and edge contributions in the expanding nanosheet structure. $SLI(G)$ also shows strong increasing behavior with large successive increments, although its growth remains slightly lower than that of $RLI(G)$. $ISLI(G)$ remains comparatively smaller throughout the range of s and t and increases smoothly because of its balanced dependence on inverse and logarithmic degree terms. $MLI(G)$

https://doi.org/10.71058/jodac.v10i05011

and $MIRI(G)$ occupy the middle range and display steady growth with moderate increments as the structural connectivity increases systematically. $MLSI(G)$ exhibits very steep growth and attains high values due to its strong amplification of higher-degree vertex contributions, making it highly sensitive to structural expansion. In contrast, $MII(G)$ remains among the smallest indices and grows slowly with only gradual, stepwise changes because its formulation reduces the dominance of high-degree vertices. $MRI(G)$ attains medium-to-large values and increases consistently, exceeding $MLI(G)$ and $MIRI(G)$, but its growth remains less aggressive than that of $RLI(G)$ and $MLSI(G)$. In the $3D$ graphical representation, the steeper surfaces correspond to indices with stronger sensitivity toward increasing structural density and connectivity, whereas flatter surfaces indicate slower and more stable growth behavior. Overall, the graph confirms that all indices are positively correlated with the increasing size, edge density, and complexity of the Octa Graphdine Nanosheet network.

Table 5: Calculated Bond Additive numerical value

(s, t)	$RLI(G_2)$	$SLI(G_2)$	$ISLI(G_2)$	$MLI(G_2)$	$MLSI(G_2)$	$MII(G_2)$	$MIRI(G_2)$	$MRI(G_2)$
(1, 1)	21	52	15	6	12	3	2	5
(2, 2)	57	135	39	16	29	7	5	13
(3, 3)	112	258	72	29	52	12	9	23
(4, 4)	184	418	116	45	81	19	15	36
(5, 5)	273	617	171	65	116	27	21	51
(6, 6)	380	855	236	88	157	36	28	69
(7, 7)	505	1131	312	114	203	47	36	89
(8, 8)	648	1446	398	143	256	59	46	112
(9, 9)	808	1799	495	175	314	72	56	137
(10, 10)	986	2190	602	211	378	87	67	165

https://doi.org/10.71058/jodac.v10i05011

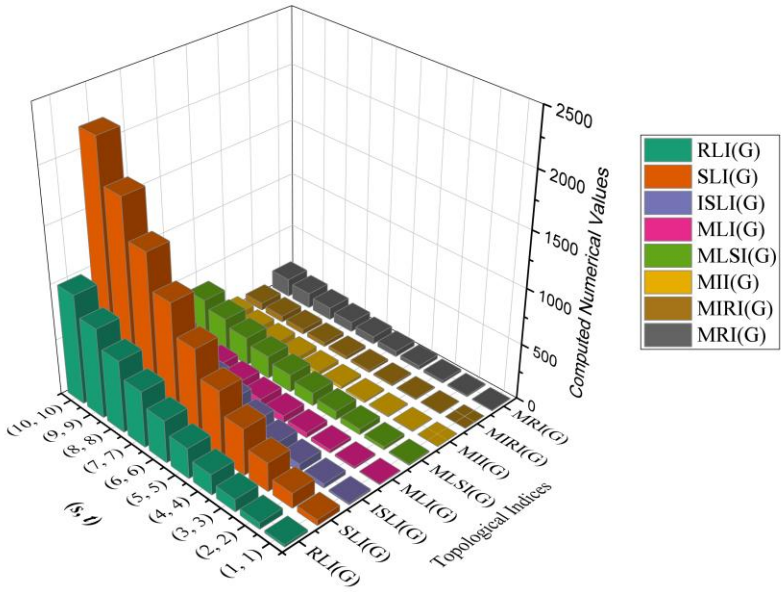

Figure 5: A visual representation of molecular characteristics for bond addition of Octa Graphdine Nanosheet

Table 6: Calculated Bond Additive numerical value

(s, t)	$MDI(G_2)$	$MHI(G_2)$	$MMRI(G_2)$	$MMRDI(G_2)$	$MMDI(G_2)$	$MMSDI(G_2)$	$SDDI(G_2)$
(1, 1)	16	2	25	32	36	48	59
(2, 2)	40	5	65	81	92	122	151
(3, 3)	72	9	123	152	172	226	284
(4, 4)	112	14	199	245	276	360	459
(5, 5)	160	20	295	360	404	524	675
(6, 6)	216	27	408	497	556	718	932
(7, 7)	280	35	541	655	732	942	1231
(8, 8)	352	44	691	835	932	1196	1571
(9, 9)	432	54	861	1037	1156	1480	1952
(10, 10)	520	65	1049	1261	1404	1794	2375

https://doi.org/10.71058/jodac.v10i05011

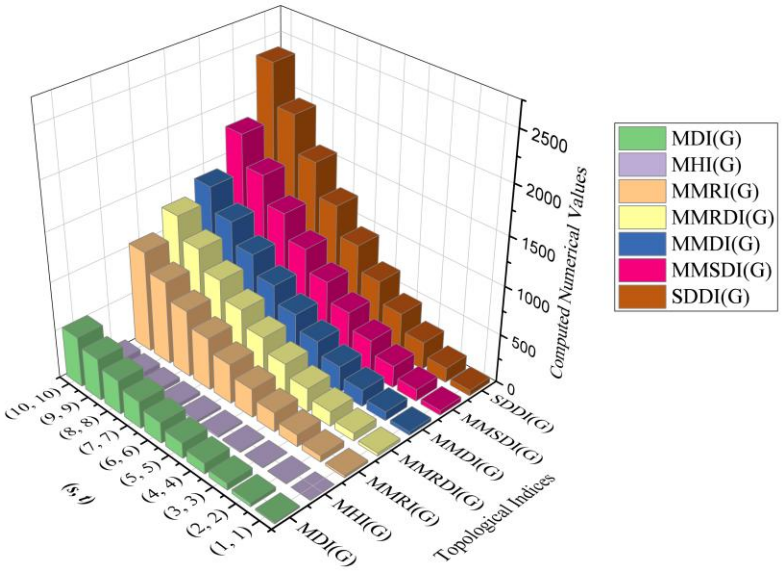

Figure 6: A visual representation of molecular characteristics for bond addition of Octa Graphdine Nanosheet

The behavior of the indices as depicted in Figure 6 can be explained using the corresponding numerical values presented in Table 6. As the parameters s and t increase, all seven bond-additive topological indices of the Octa Graphdine Nanosheet O_2 $G_{(s\times t)}$ increase monotonically, but with clearly different magnitudes and growth rates. $MDI(G)$ exhibits rapid growth from moderate values to comparatively large values because it strongly depends on increasing vertex degrees and edge contributions in the expanding nanosheet structure. $MHI(G)$ remains the smallest index throughout the considered range and increases slowly with only small successive increments due to its harmonic type reciprocal degree formulation, which reduces the influence of high-degree vertices. $MMRI(G)$ lies in the lower-to-middle range and grows smoothly with gradual increments, indicating moderate sensitivity toward structural expansion and connectivity changes. $MMRDI(G)$ occupies a middle range and shows steady accelerating growth that is stronger than $MMRI(G)$ but weaker than the highly sensitive SD-type indices. $MMDI(G)$ exhibits comparatively strong growth and attains large values at higher s and t, reflecting its dependence on multiplicative degree interactions within the network. $MMSDI(G)$ is among the largest and fastest-growing indices, showing steep successive increments and very high sensitivity toward increasing edge density and structural complexity of the nanosheet. $SDDI(G)$ also displays rapid growth and attains high values, exceeding all middle-range indices and growing nearly as aggressively as $MMSDI(G)$. In the $3D$ graphical representation, the steeper surfaces correspond to indices with stronger dependence on higher-order degree interactions and structural density, whereas flatter surfaces indicate slower and more stable growth behavior. Overall, the graph confirms that all seven indices are strongly correlated with the increasing size, connectivity, and complexity of the Octa Graphdine Nanosheet network.

https://doi.org/10.71058/jodac.v10i05011

3 Conclusion

In this paper, some degree based bond additive indices related to nanosheets made up of Octa Graphene structures such as Octa Grayphyne and Octa Graphdine are rigorously investigated. These calculated expressions give insight into the nature and various aspects of these structures, i.e., their physical and chemical stability as well as biological activity. The studied topological indices have a significant importance regarding theoretical study of nanostructures and can be utilized effectively in the area of QSAR and QSPR analysis. Moreover, the presented calculations help to gain more insight into the physical and electronic nature of these nanostructures, which would be very helpful for designing future devices made out of these materials, such as nano electronic circuits, nano batteries, and drug delivery systems.

References

[1] W.U. Jing, Y. S. Wang, X.Y. Yang et al., Graphene oxide used as a carrier for adriamycin can reverse drug resistance in breast cancer cells, Nanotechnology, vol. 23, no. 35, Article ID 355101, 2012.

[2] D. Golberg, Y. Bando, O. Stephan, and K. Kurashima, Octahedral boron nitride fullerenes formed by electron beam irradiation, Applied Physics Letters, vol. 73, pp. 2441-2443, 1998.

[3] M. V. Diudea, â€œNanostructures, Novel Architecture, NOVA, New York, NY, USA, 2005.

[4] G.S.L. Fabris, C.A. Paskocimas, J.R. Sambrano, and R. Paupitz, New 2D nanosheets based on the octa-graphene, Journal of Solid State Chemistry, vol. 290, Article ID 121534, 2020.

[5] H. Weiner, Structural determination of parrafin boiling point, Journal of the American Chemical Society, vol. 69, no. 1, pp. 17-20, 1947.

[6] N. Trinajstic, Chemical graph theory, CRC Press, Boca Raton, FL., 1992.

[7] R. Todeschini, V. Consonni, Handbook of molecular descriptors, Wiley, 2000.

[8] H.Y. Azari, M.H. Khalifeh, A.R. Ashra, Calculating the edge Wiener and Szeged indices of graphs, J. Comput. Appl. Math. vol. 235, pp. 4844-4870, 2011.

[9] D. Vukicevic, M. Gasperov, Bond aditive modelling 1, Ariatic indices, Croat. Chem. Acta., vol. 83, pp. 243-240, 2010.

[10] S. Prabhu, G. Murugan and K.S. Sudhakhar, On the new topological index of certain nanostructures using combinatorial computation, J. Comp. Math. Sci., vol. 9, pp. 1257-1245, 2018.

[11] Gunasekar, T. Kathavarayan, P. Murugan, G. Julietraja, K.; On Certain Degree Based and Bond Additive Molecular Descriptors of Hexabenzocorenene.*Biointerface Res. Appl.*

https://doi.org/10.71058/jodac.v10i05011

Chem. , vol. 13, pp. 2970-2987, 2023.

[12] Gunasekar, T. Kathavarayan, P. Alsinai, A. Murugan, G. On Certain Degree Based and Bond-Additive Topological Indices of Dodeca-Benzo-Circumcorenene, Combinatorial Chemistry & High Throughput Screening, DOI: 10.2174/0113862073274943231211110011.

[13] Y. Hu, X. Li, Y. Shi, T. Xu, and I. Gutman, On molecular graphs with smallest and greatest zeroth-Corder general Randic index, MATCH Communications in Mathematical and in Computer Chemistry, vol. 54, pp. 425-434, 2005.

[14] M. Randic, On Characterization of molecular branching, Journal of the American Chemical Society, vol. 97, pp. 6609-6615, 1975.

[15] S. Kanwal, S. Shang, M. K. Siddiqui, T. S. Shaikh, A. Afzal, and A. T. Anton, On analysis of topological aspects of subdivision of kragujevac tree networks, Mathematicle Problems In Engineering, vol. 2021, Article ID 9082320, 15 pages, 2021.

[16] S Nasir, FB Farooq, N Idrees, MJ Saif, and F. Saeed, Topological characterization of nanosheet covered by C3 and C6, Processes, vol. 7, no. 7, 2019.

[17] S. Kanwal, A. Riyasat, M. K. Siddiqui et al., On topological indices on total graphs and its line graph for kragujevac tree networks, Complexity, vol. 2021, Article ID 8695121, 32 pages, 2021.

[18] M. Munir, W. Nazeer, S. Rafique, and S. M. Kang, M- polynomial and degree-based topological indices of polyhex nanotubes, Symmetry, vol. 8, 2016.

[19] M. S. Ahmad, W. Nazeer, S. M. Kang, and C. Y. Jung, M- polynomials and degree based topological indices for the line graph of firecracker graph, Global Journal Of Pure And Applied Mathematics, vol. 13, pp. 2749-2776, 2017.

[20] Fozia Bashir Farooq, Topological Properties of Nano Sheets Based on Octa Graphene, Journal of Mathematics, Article ID 2106974, 2022.